

Role of knockout contributions in giant resonance studies with $(p,p'x)$ reactions

J. Carter,¹ A. A. Cowley,² H. Diesener,^{3,*} R. W. Fearick,⁴ S. V. Förtsch,⁵ J. J. Lawrie,⁵ P. von Neumann-Cosel,³ J. V. Pilcher,⁵ A. Richter,³ K. Schweda,^{3,†} F. D. Smit,⁵ G. F. Steyn,⁵ and S. Strauch^{3,‡}

¹Physics Department, University of the Witwatersrand, PO Wits, Johannesburg 2050, South Africa

²Physics Department, University of Stellenbosch, Private Bag XI, Matieland 7602, South Africa

³Institut für Kernphysik, Technische Universität Darmstadt, D-64289 Darmstadt, Germany

⁴Physics Department, University of Cape Town, Rondebosch 7700, South Africa

⁵National Accelerator Centre, Faure 7131, South Africa

(Received 3 November 2000; published 16 April 2001)

The giant-resonance region in ^{40}Ca and ^{48}Ca has been studied using the reactions $^{48}\text{Ca}(p,p'n_0)^{47}\text{Ca}$, $^{40}\text{Ca}(p,p'p_0)^{39}\text{K}$, and $^{40}\text{Ca}(p,p'\alpha_0)^{36}\text{Ar}$ for an incident proton energy $E_p=100$ MeV. Knockout cross sections for these reactions were calculated within the distorted wave impulse approximation formalism using parameters fixed from previous investigations. The results quantitatively account for the data at higher excitation energies while the knockout contributions underneath the main resonance strength are small.

DOI: 10.1103/PhysRevC.63.057602

PACS number(s): 24.50.+g, 25.40.Ep, 27.40.+z

Giant-resonance excitation and decay has been studied extensively [1,2]. In particular, recent notable progress has been the observation of a strong fragmentation of the isoscalar giant-resonance strengths in medium-mass nuclei [3–6]. A powerful experimental tool is the measurement of angular correlations, whereby the inelastically scattered probe is detected in coincidence with a light decay particle or cluster (usually neutrons, protons, or α particles). By fitting an angular correlation function to the data, a multipole strength decomposition can, in principle, be accomplished for the various resolved decay channels. For example, a forward/backward asymmetry is a sensitive indicator of even small admixtures of odd/even multipoles. Unfortunately, in hadronic reactions the presence of a competing knockout process leads also to the same effect and great care has to be taken to subtract a background from angular correlation data measured near the recoil direction of the heavy nucleus [7].

Nucleon and cluster knockout reactions have been studied extensively both experimentally and theoretically (see, e.g., Refs. [8–11]). Reactions of particular interest have been of the type $(\alpha,2\alpha)$, $(p,p'n)$, $(p,p'p)$, and $(p,p'\alpha)$ on $1p$, $2s1d$, and $1f_{7/2}$ shell-model nuclei. The theoretical analysis of these knockout reactions has been accomplished very successfully by using the distorted wave impulse approximation (DWIA). On the experimental side, most of the data reported were for the condition of quasifree scattering (angle pairs at which zero recoil momentum of the residual nucleus is kinematically allowed). It has been pointed out though that data taken at nonquasifree angle pairs could be sensitive to off-shell effects [12]. This is particularly so when the scattered projectile carries most of the kinetic energy resulting from probing the high momentum part of the wave function of the

struck nucleon/cluster. Thus, the question remains to what extent these models hold for kinematical conditions that are optimized to enhance the giant-resonance cross sections, but are at rather extreme limits for the knockout process.

In the present work an extensive set of angular correlations for the reactions $^{40}\text{Ca}(p,p'p)^{39}\text{K}$, $^{40}\text{Ca}(p,p'\alpha)^{36}\text{Ar}$, and $^{48}\text{Ca}(p,p'n)^{47}\text{Ca}$ at $E_p=100$ MeV is presented aiming at a study of the isoscalar giant quadrupole resonance in ^{40}Ca and ^{48}Ca that is present at low excitation energies. However, in order to extract reliable multipole strengths from the fitted angular correlations, a knowledge of the background knockout cross section is crucial.

A series of experiments using a 100 MeV proton beam were performed at the cyclotron facility of the National Accelerator Center, Faure, South Africa. The inelastically scattered protons were detected by means of the K600 magnetic spectrometer. Data were taken for $^{40,48}\text{Ca}$ excitation energies $E_x \approx 10\text{--}23$ MeV. Targets of $^{\text{nat}}\text{Ca}$ were used for the $^{40}\text{Ca}(p,p'p)$ and $(p,p'\alpha)$ reactions. Charged particle emission by the excited ^{40}Ca was observed using a set of three $\Delta E-E$ semiconductor telescopes mounted on a turntable in the scattering chamber, permitting the measurement of complete angular correlations. Typical energy spectra for the p_0 and α_0 channels are shown in the middle and lower parts, respectively, of Fig. 1. More details of the experimental setup can be found in Ref. [13].

In a separate experiment a highly enriched ^{48}Ca (92.5%) target was used to measure the $^{48}\text{Ca}(p,p'n)$ reaction. The angular correlations were obtained by employing an array of six organic liquid scintillators [6] to detect the emitted neutrons with the neutron kinetic energy determined using the time-of-flight technique. A typical energy spectrum for the n_0 channel is shown in the upper part of Fig. 1. In both experiments the choice of the scattering angle of the inelastically scattered proton from $^{40,48}\text{Ca}$ was determined by the need to excite strongly low-lying isoscalar giant multipoles in the target nuclei (see Ref. [13]). An extensive set of data has been measured for each fixed scattering angle θ_p , by varying $\theta_{x=n_0,p_0,\alpha_0}$, where these angles on the opposite side

*Present address: EDS, D-63037 Offenbach, Germany.

†Present address: Lawrence Berkeley National Laboratory, 1 Cyclotron Road, Berkeley, CA 94720.

‡Present address: Department of Physics and Astronomy, Rutgers University, Piscataway, NJ 08854.

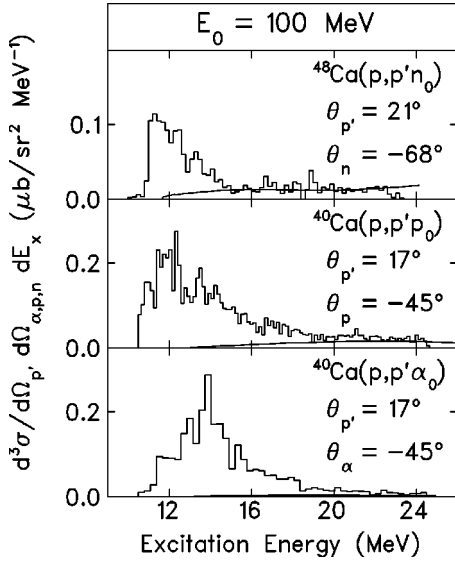


FIG. 1. Examples of measured cross sections (histograms) for the reactions $^{48}\text{Ca}(p,p'n)^{47}\text{Ca}$, $^{40}\text{Ca}(p,p'p_0)^{39}\text{K}$, and $^{40}\text{Ca}(p,p'\alpha_0)^{36}\text{Ar}$ as a function of excitation energy together with the results of the DWIA calculations (solid lines) described in the text. The knockout process involves the $1f_{7/2}$, $1d_{3/2}$, and $5s$ orbitals for the three reactions, respectively.

of the incident beam are referred to throughout as negative scattering angles. In all cases the features displayed in the energy spectra measured for each channel are as shown in Fig. 1.

The main resonant cross section lies below $E_x(^{40,48}\text{Ca}) \approx 16$ MeV and has been described previously as giant-resonance excitation and decay [13,14]. However, of particular importance is an understanding of the long tail in the respective energy spectra extending up to the highest excitation energies measured. If these cross sections could be attributed to isoscalar giant resonances, they would provide a clear signature of significant direct decay components, as were observed for the isovector giant dipole resonance in these nuclei [4,6,15]. However, this high-energy tail may also arise from knockout reactions. Furthermore, as pointed out above, a quantitative knowledge of the knockout contributions underneath the main giant-resonance part is essential for an analysis of the angular correlations. Thus, the present data are used as a test case of the model description of the knockout reactions for cases far from the condition of quasi-free kinematics.

The method of analysis of these types of reactions within a factorized DWIA has been presented in detail in the literature [8,16,17]. For the sake of brevity only the most salient features are described here. The discussion is limited to the non-spin-orbit case. Inclusion of a spin-orbit term in the interaction potentials leads to more complicated equations but the main features remain.

The cross section for a reaction $A(a,a'b)B$ can be written as [16]

$$\frac{d^3\sigma}{d\Omega_{a'}d\Omega_b dE_{a'}} = S_b F_K \frac{d\sigma}{d\Omega_{a+b}} \sum_{\Lambda} |T_L^{\Lambda}|^2, \quad (1)$$

where S_b is the spectroscopic factor for the bound nucleon/cluster b , F_K is a kinematic factor, and $d\sigma/d\Omega_{a+b}$ is the half-shell cross section for $a+b$ scattering. The distorted momentum distribution for the particle/cluster b bound to core B in the target A is given by

$$T_L^{\Lambda} = (2L+1)^{-1/2} \times \int \chi_{a'}^{(-)*}(\mathbf{r}) \chi_b^{(-)*}(\mathbf{r}) \Phi_L^{\Lambda}(\mathbf{r}) \chi_a^{(+)*} \left[\frac{M_B \mathbf{r}}{M_A} \right] d\mathbf{r}. \quad (2)$$

Here, the χ 's are the distorted waves for the incident and emitted particles, and $\Phi_L^{\Lambda}(\mathbf{r})$ is the relative-motion wave function for b orbiting core B (mass M_B) in the target A (mass M_A).

Suitable optical potentials valid within the kinematic range of the experimental data are required for the evaluation of the distorted waves χ . These take the usual form of a real plus imaginary volume Woods-Saxon term, a surface derivative imaginary term, and a real plus imaginary spin-orbit term.

The following potentials were used: (1) For the incident channels $p + ^{40,48}\text{Ca}$ at $E_p = 100$ MeV the optical potential parameters of Schwandt *et al.* [18]. (2) Again the Schwandt *et al.* [18] potential is suitable for describing the inelastically scattered protons up to excitation energies $E_x = 23$ MeV, i.e., in the energy region $77 \text{ MeV} < E_{p'} < E_p - s_b$, where s_b is the corresponding separation energy for a neutron (9.95 MeV), proton (8.33 MeV), or α particle (7.04 MeV) knocked out. (3) The knocked-out particles b emerge with kinetic energies $0 < E_b < E_p - E_{p'} - s_b$ where (i) for the n_0 channel $^{48}\text{Ca}(p,p'n_0)^{47}\text{Ca}$, $0 < E_{n_0} < 13$ MeV, the neutron potential of Becchetti and Greenless [19] was applied, (ii) for the p_0 channel $^{40}\text{Ca}(p,p'p_0)^{39}\text{K}$, $0 < E_{p_0} < 16.7$ MeV, the proton potential of Becchetti and Greenless [19] (with a geometry similar to the neutron potential) was chosen, and (iii) for the α_0 channel $^{40}\text{Ca}(p,p'\alpha_0)^{36}\text{Ar}$, $0 < E_{\alpha_0} < 18$ MeV, the α -particle potential of Huizenga and Igo [20] was used. The various bound-state potential parameters employed were ($n + ^{47}\text{Ca}$) [21], ($p + ^{39}\text{K}$) [22], and ($\alpha + ^{36}\text{Ar}$) [23]. These potentials again take the usual form and include a real central part and a spin-orbit term as required.

The calculations were performed using the DWIA code THREEDEE [8,17]. No fitting of the predictions to the experimental data was attempted. In this regard, the spectroscopic factors S_b used to obtain absolute cross sections for the n_0 and α_0 channel were fixed from previous investigations ($S_{n_0} = 7.0$ [9] and $S_{\alpha_0} = 0.83$ [10]). In the case of the p_0 channel the shell-model limit of $S_{p_0} = 4.0$ for protons knocked out of the $1d_{3/2}$ shell was used.

As examples, the triple-differential cross sections are shown for the spectra of Fig. 1. In all three reactions the energy dependence is well described at higher excitation energies ($E_x \geq 16$ MeV in ^{40}Ca , $E_x \geq 14$ MeV in ^{48}Ca). In particular for the nucleon knockout, the DWIA results quantitatively account for the measured cross sections in this energy region indicating knockout reactions to be the dominant

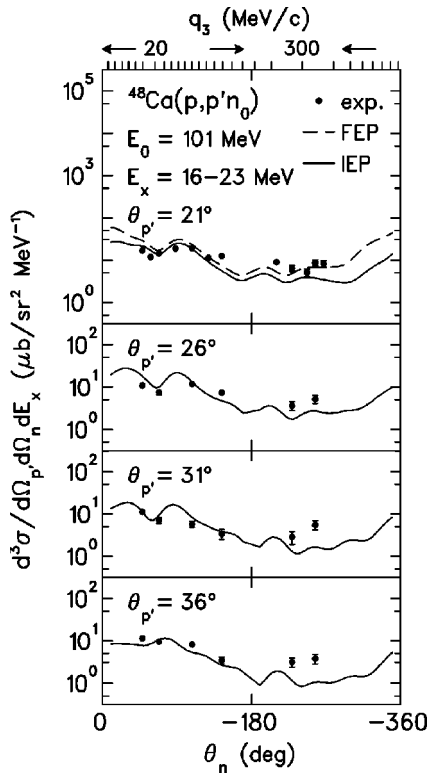


FIG. 2. Angular correlation cross sections for the reaction $^{48}\text{Ca}(p,p'n_0)^{47}\text{Ca}$ in the excitation energy range $E_x(^{48}\text{Ca}) = 16\text{--}23$ MeV together with results of the DWIA cross section predictions for the initial energy prescription (IEP, solid lines) and the final energy prescription (FEP, dashed line) described in the text. The top axis shows the recoil momentum q_3 of the heavy residual nucleus for the smallest proton scattering angle.

process. For the α_0 decay, the calculations are systematically below the data. Towards lower E_x the knockout predictions decrease smoothly and contributions under the main bump of the resonance cross sections are very small.

The angular dependence for the n_0 channel in the excitation energy window $E_x(^{48}\text{Ca}) = 16\text{--}23$ MeV together with the DWIA predictions are presented in Fig. 2. Here, the recoil momentum q_3 of the heavy core can be obtained for the smallest p' scattering angle from the axis shown on the top part of the figure where it can be seen that most points correspond to nonquasifree angle pairs, i.e., the heavy residual nucleus recoil momentum is not zero. Similarly, the results for the p_0 channel, but in an excitation energy window $E_x(^{40}\text{Ca}) = 20\text{--}23$ MeV, together with the corresponding DWIA predictions are shown in Fig. 3. As can be seen, in both reactions there is a very good correspondence between the measured cross sections and the DWIA calculations, even at scattering angle pairs far from the quasifree condition. For the α_0 channel displayed in Fig. 4 the prediction of the calculation does not exceed the measured cross section at any emission angle. It should be emphasized again that all parameters in the DWIA calculations are fixed. The knockout scattering is thus interpreted as a small nonresonant background on top of which lies the decay of the giant-resonance strength excited in the target nucleus. As such, the

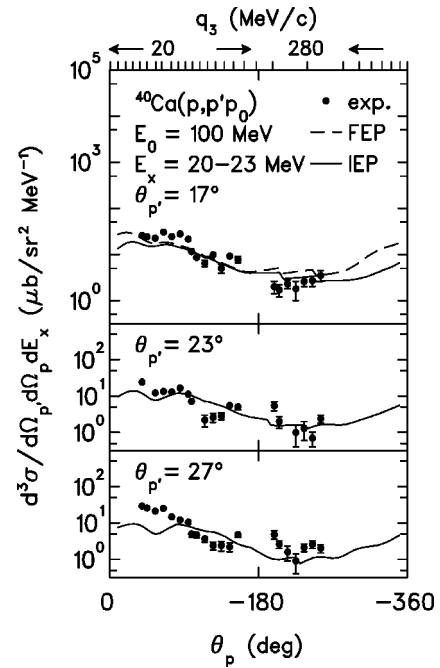


FIG. 3. Same as Fig. 2 but for the reaction $^{40}\text{Ca}(p,p'p_0)^{39}\text{K}$ and an excitation energy range $E_x(^{40}\text{Ca}) = 20\text{--}23$ MeV.

knockout part under the resonant yield does not significantly affect the analysis of the angular correlations [14].

In common with most knockout studies, we avoid the complication of the need for a half-shell two-body cross section by introducing an on-shell approximation. This procedure requires though the choice of an on-shell energy prescription. For example, one could evaluate the two-body cross section at either the initial (referred to as the initial

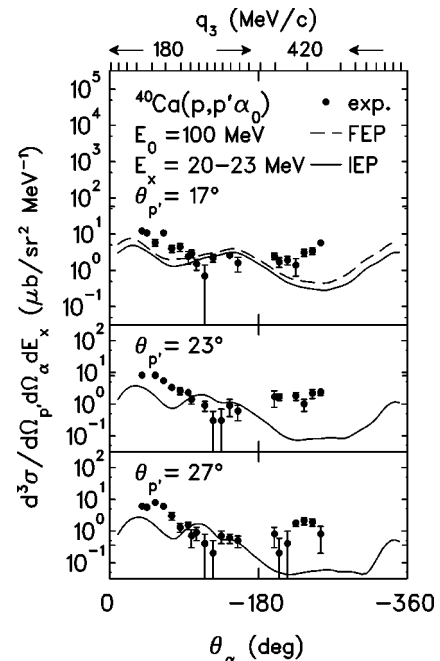


FIG. 4. Same as Fig. 2 but for the reaction $^{40}\text{Ca}(p,p'\alpha_0)^{36}\text{Ar}$ and an excitation energy range $E_x(^{40}\text{Ca}) = 20\text{--}23$ MeV.

energy prescription, IEP) or final relative nucleon-nucleon energies (final energy prescription, FEP). Of course, a proper half-shell cross section is expected to correspond to a value somewhere between that resulting from the two extreme prescriptions. The results presented are for the IEP but the FEP distributions are qualitatively similar (see dashed lines in Figs. 2–4). Even better agreement would be obtained if adjustments (within accepted uncertainties) were to be made to the spectroscopic factors. One may also note that a comparison of different choices of the optical model for the knocked-out particle leads to variations of the cross sections of the same order of magnitude.

To conclude, an extensive set of data measured for the reactions $^{48}\text{Ca}(p,p'n_0)^{47}\text{Ca}$, $^{40}\text{Ca}(p,p'p_0)^{39}\text{K}$, and $^{40}\text{Ca}(p,p'\alpha_0)^{36}\text{Ar}$ has been used to test the reliability of the DWIA model to describe the knockout contributions to the cross sections for kinematics far from the quasifree limit at

incident energies where off-shell effects should be non-negligible. Despite neglecting the latter, encouraging results are obtained. At higher excitation energies away from the main resonant strength the energy dependence of the cross sections can be reproduced well. Also, a reasonable quantitative description is achieved for the nucleon emission channels over a range of relative momentum between the scattered proton and the knocked-out particle. For the α emission case the calculations are systematically below the data suggesting the presence of resonance excitations even at high excitation energies. An extrapolation of the knockout cross sections suggests very small contributions at lower excitation energies where the main resonance strength resides.

The authors acknowledge support by the NRF, South Africa and by the DFG under Contract No. FOR 272/2-1. We thank D. Frekers for the loan of the precious ^{48}Ca target.

-
- [1] *Electric and Magnetic Giant Resonances in Nuclei*, edited by J. Speth (World Scientific, Singapore, 1991).
- [2] P. F. Bortignon, A. Bracco, and R. A. Broglia, *Giant Resonances: Nuclear Structure at Finite Temperature* (Harwood Academic, Amsterdam, 1998).
- [3] F. Zwarts, A. G. Drentje, M. N. Harakeh, and A. van der Woude, Nucl. Phys. **A439**, 117 (1985).
- [4] H. Diesener, U. Helm, G. Herbert, V. Huck, P. von Neumann-Cosel, C. Rangacharyulu, A. Richter, G. Schrieder, A. Stascheck, A. Stiller, J. Ryckebusch, and J. Carter, Phys. Rev. Lett. **72**, 1994 (1994).
- [5] D. H. Youngblood, H. L. Clark, and Y.-W. Lui, Phys. Rev. C **55**, 2811 (1997).
- [6] S. Strauch, P. von Neumann-Cosel, C. Rangacharyulu, A. Richter, G. Schrieder, K. Schweda, and J. Wambach, Phys. Rev. Lett. **85**, 2913 (2000).
- [7] See, e.g., K. T. Knöpfle and G. J. Wagner, in *Electric and Magnetic Giant Resonances* (Ref. [1]), p. 236, and references therein.
- [8] N. S. Chant, P. Kitching, P. G. Roos, and L. Antonuk, Phys. Rev. Lett. **43**, 495 (1979).
- [9] J. W. Watson, M. Ahmed, D. W. Devins, B. S. Flanders, D. L. Friesel, N. S. Chant, P. G. Roos, and J. Wastell, Phys. Rev. C **26**, 961 (1982).
- [10] A. Nadasen, P. G. Roos, N. S. Chant, A. A. Cowley, C. Samanta, and J. Wesick, Phys. Rev. C **23**, 2353 (1981).
- [11] C. Samanta, N. S. Chant, P. G. Roos, A. Nadasen, J. Wesick, and A. A. Cowley, Phys. Rev. C **34**, 1610 (1986).
- [12] E. F. Redish, G. J. Stephenson, Jr., and G. M. Lerner, Phys. Rev. C **2**, 1665 (1970).
- [13] J. Carter, A. A. Cowley, H. Diesener, R. W. Fearick, S. V. Försch, J. J. Lawrie, S. J. Mills, P. von Neumann-Cosel, M. N. Harakeh, R. T. Newman, J. V. Pilcher, A. Richter, K. Schweda, F. D. Smit, G. F. Steyn, S. Strauch, and D. M. Whittall, Nucl. Phys. **A630**, 631 (1998).
- [14] K. Schweda, J. Carter, H. Diesener, R. W. Fearick, S. V. Försch, J. J. Lawrie, P. von Neumann-Cosel, J. V. Pilcher, A. Richter, F. D. Smit, G. F. Steyn, and S. Strauch, Phys. Lett. B (in press).
- [15] J. Carter, H. Diesener, U. Helm, G. Herbert, P. von Neumann-Cosel, A. Richter, G. Schrieder, and S. Strauch, Nucl. Phys. A (submitted).
- [16] N. S. Chant and P. G. Roos, Phys. Rev. C **15**, 57 (1977).
- [17] N. S. Chant and P. G. Roos, Phys. Rev. C **27**, 1060 (1983).
- [18] P. Schwandt, H. O. Meyer, W. W. Jacobs, A. D. Bacher, S. E. Vigdor, M. D. Kaitchuck, and T. R. Donoghue, Phys. Rev. C **26**, 55 (1982).
- [19] F. D. Becchetti, Jr. and G. W. Greenless, Phys. Rev. **182**, 1190 (1969).
- [20] J. R. Huizenga and G. Igo, Nucl. Phys. **29**, 462 (1962).
- [21] C. J. Batty and G. W. Greenless, Nucl. Phys. **A133**, 673 (1969).
- [22] R. L. B. Elton and A. Swift, Nucl. Phys. **A94**, 52 (1967).
- [23] N. Anantaraman, C. L. Bennett, J. P. Draayer, H. W. Fulbright, H. E. Gove, and J. Töke, Phys. Rev. Lett. **35**, 1131 (1975).